CrossMark

A two-step linear programming model for energy-efficient timetables in metro railway networks

Shuvomoy Das Gupta [a,*], J. Kevin Tobin [b], Lacra Pavel [a]

[a] Department of Electrical & Computer Engineering, University of Toronto, 10 King's College Road, Toronto, Ontario, Canada
[b] Thales Canada Inc., 105 Moatfield Drive, Toronto, Ontario, Canada

ARTICLE INFO

ABSTRACT

In this paper we propose a novel two-step linear optimization model to calculate energy-efficient timetables in metro railway networks. The resultant timetable minimizes the total energy consumed by all trains and maximizes the utilization of regenerative energy produced by braking trains, subject to the constraints in the railway network. In contrast to other existing models, which are $\mathcal{NP}$-hard, our model is computationally the most tractable one being a linear program. We apply our optimization model to different instances of service PES2-SFM2 of line 8 of Shanghai Metro network spanning a full service period of one day (18 h) with thousands of active trains. For every instance, our model finds an optimal timetable very quickly (largest runtime being less than 13 s) with significant reduction in effective energy consumption (the worst case being 19.27%). Code based on the model has been integrated with `Thales Timetable Compiler` - the industrial timetable compiler of Thales Inc that has the largest installed base of communication-based train control systems worldwide.

1. Introduction

1.1. Background and motivation

Efficient energy management of electric vehicles using mathematical optimization has gained a lot of attention in recent years (Bashash et al., 2011; Mura et al., 2013; Nuesch et al., 2012; Patil et al., 2012; Saber and Venayagamoorthy, 2010). When a train makes a trip from an origin platform to a destination platform, its optimal speed profile consists of four phases: 1) maximum acceleration, 2) speed hold, 3) coast and 4) maximum brake (Howlett and Pudney, 1995), as shown in Fig. 1 in a qualitative manner. Most of the energy required by the train is consumed during the accelerating phase. During the speed holding phase the energy consumption is negligible compared to accelerating phase, and during the coasting phase there is no need for energy. When the train brakes, it produces energy by using a regenerative braking mechanism. This energy is called regenerative braking energy. Calculating energy-efficient timetables for trains in railway networks is a relevant problem in this regard. Electricity is the main source of energy for trains in most modern railway networks; in such networks, a train is equipped with a regenerative braking mechanism that allows it to produce electrical energy during its braking phase. In this paper, we formulate a two-step linear optimization model to obtain an energy-efficient timetable

---

* Corresponding author.
   E-mail addresses: shuvomoy.dasgupta@mail.utoronto.ca (S.D. Gupta), Kevin.Tobin@thalesgroup.com (J.K. Tobin), pavel@control.utoronto.ca (L. Pavel).
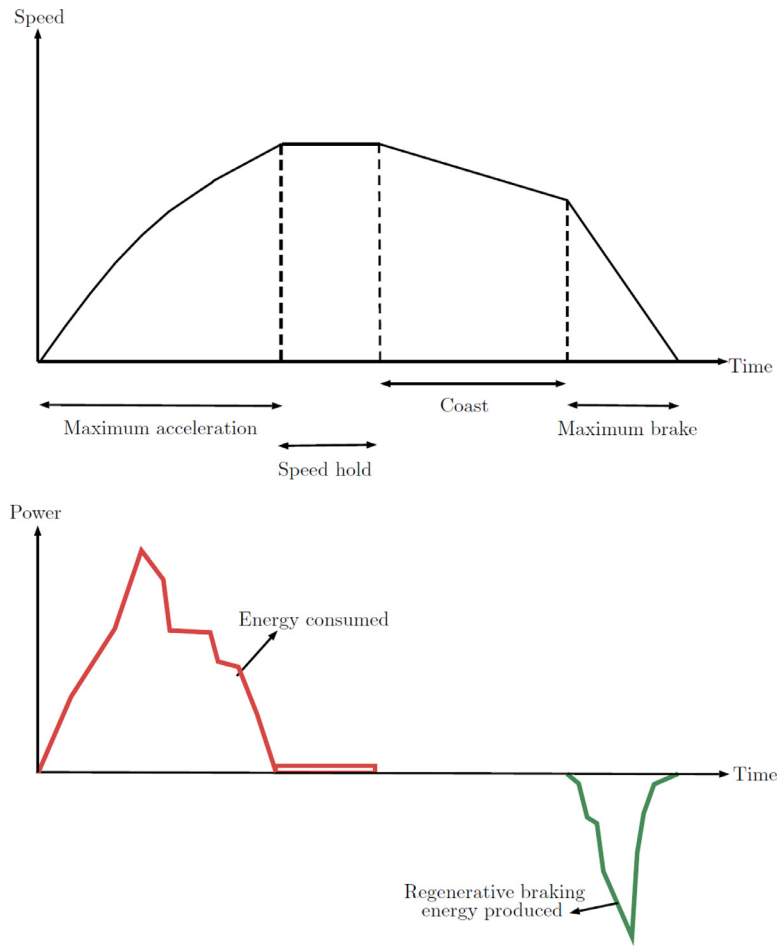
Fig. 1. Optimal speed profile of a train.

for a metro railway network. The timetable schedules the arrival time and the departure time of each train to and from the platforms it visits such that the total electrical energy consumed is minimized and the utilization of produced regenerative energy is maximized.

1.2. Related work

The general timetabling problem in a metro railway network has been studied extensively over the past three decades (Harrod, 2012). However, very few results exist that can calculate energy-efficient timetables. Now we discuss the related research. We classify the related work as follows. The first two papers are mixed integer programming model, the next three are models based on meta-heuristics and the last one is an analytical study.

A Mixed Integer Programming (MIP) model, applicable only to single train-lines, is proposed by Peña-Alcaraz et al. (2012a) to maximize the total duration of all possible synchronization processes between all possible train pairs. The model is then applied successfully to line three of the Madrid underground system. However, the model can have some drawbacks. First, considering all train pairs in the objective will result in a computationally intractable problem even for a moderate sized railway network. Second, for a train pair in which the associated trains are far apart from each other, most, if not all, of the regenerative energy will be lost due to the transmission loss of the overhead contact line. Finally, the model assumes that the durations of braking and accelerating phases stay the same with varying trip times, which is not the case in reality.

The work in Das Gupta et al. (2015) proposes a more tractable MIP model, applicable to any railway network, by considering only train pairs suitable for regenerative energy transfer. The optimization model is applied numerically to the Dockland Light Railway and shows a significant increase in the total duration of the synchronization process. Although such increase, in principle, may increase the total savings in regenerative energy, the actual energy saving is not directly addressed. Similar to Peña-Alcaraz et al. (2012a), this model too, assumes that even if the trip time changes, the duration of the associated braking and accelerating stay the same.
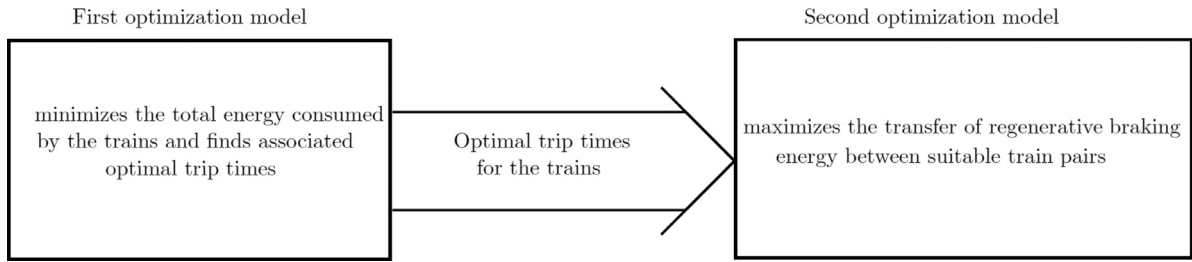
First optimization model

Second optimization model

minimizes the total energy consumed by the trains and finds associated optimal trip times

Optimal trip times for the trains

maximizes the transfer of regenerative braking energy between suitable train pairs

Fig. 2. Flow-chart of the two steps of the optimization model.

Other relevant works implement meta-heuristics. The work in Li and Lo (2014a) implements genetic algorithm to calculate timetables that maximize the utilization of regenerative energy while minimizing the tractive energy of the trains. Numerical studies for the model is implemented to Beijing Metro Yizhuang Line of China showing notable increase in energy efficiency. The work in Yang et al. (2013) presents a cooperative integer programming model to utilize the use of regenerative energy of trains and proposes genetic algorithm to solve it. Similar to Li and Lo (2014a), this numerical studies have been performed to Beijing Metro Yizhuang Line of China, though the improvement is stated in the increase in overlapping time only. The work in Le et al. (2014) presents a nonlinear integer programming model which is solved using simulated annealing. The numerical experiments have been conducted for the island line of the mass transit system in Hong Kong.

An insightful analytical study of a periodic railway schedule appears in Li and Lo (2014b). The model uses the KKT conditions to calculate and analyze the properties of an energy-efficient timetable. The resultant analytical model is then applied to Beijing Metro Yizhuang Line of China numerically, which shows that the model can reduce the net energy consumption considerably.

1.3. Contributions

We propose a novel two-step linear optimization model to calculate an energy-efficient railway timetable. The *first* optimization model minimizes the total energy consumed by all trains subject to the constraints present in the railway network. The problem can be formulated as a linear program, with the optimal value attained by an integral vector. The *second* optimization model uses the optimal trip time from the first optimization model and maximizes the transfer of regenerative braking energy between suitable train pairs. Both the steps of our optimization model are linear programs, whereas the optimization models in related works are $\mathcal{NP}$-hard. A flow-chart of the two steps of the optimization model is shown in Fig. 2. Our model can calculate energy-efficient railway timetables for large scale networks in a short CPU time. Code based on the model has been embedded with the railway timetable compiler (`Thales Timetable Compiler`) of Thales Inc, which has the largest installed base of communication-based train control systems worldwide. `Thales Timetable Compiler` is used by many railway management systems worldwide including: Docklands Light Railway in London, UK., the West Rail Line and Ma On Shan Line in Hong Kong, the Red Line and Green Line in Dubai, the Kelana Jaya Line in Kuala Lumpur.

This paper is organized as follows. In Section 2 we describe the notation used, and then in Section 3 we model and justify the constraints present in the railway network. The first optimization model is presented in Section 4. Section 5 formulates the second optimization problem that additionally maximizes the utilization of regenerative braking energy. Section 6 describes the limitations of the optimization model. In Section 7 we apply our model to different instances of an existing metro railway network spanning a full working day and describe the results. Section 8 presents the conclusion.

2. Notation and notions

Every set described in this paper is strictly ordered and finite unless otherwise specified. The set-cardinality (number of elements of the set) and the ith element of such a set C is denoted by $|C|$ and $C(i)$ respectively. The set of real numbers and integers are expressed by $\mathbf{R}$ and $\mathbf{Z}$ respectively; subscripts $+$ and $++$ attached with either set denote non-negativity and positivity of the elements respectively. A column vector with all components one is denoted by $\mathbf{1}$. The symbol $\preceq$ stands for componentwise inequality between two vectors and the symbol $\wedge$ stands for conjunction. The number of nonzero components of a vector x is called cardinality of that vector and is denoted by $\mathbf{card}(x)$. Note that, cardinality of a vector is different from set-cardinality. The ith unit vector e_i is the vector with all components zero except for the ith component which is one. The epigraph of a function $f: C \to \mathbf{R}$ (where C is any set) denoted by $\mathbf{epi}\, f$ is the set of input-output pairs that f can achieve along with anything above, *i.e.,*

$$\mathbf{epi}\, f = \{(x, t) \in C \times \mathbf{R} \mid x \in C, t \geq f(x)\}.$$

The convex hull of any set C, denoted by $\mathbf{conv}\, C$, is the set containing all convex combinations of points in C. Consequently, if C is nonconvex, then its best convex outer approximation is $\mathbf{conv}\, C$, as it is the smallest set containing C.

The set of all platforms in a railway network is indicated by $\mathcal{N}$. A directed arc between two distinct and non-opposite platforms is called a track. The set of all tracks is represented by $\mathcal{A}$. The directed graph of the railway network is expressed

Table 1
List of symbols.

$|C|$	The number of elements of a finite countable set C
$C(i)$	The ith element of a finite countable set C
$\mathbf{R}$	The set of real numbers
e_i	The ith unit vector
epi f	The epigraph of a function f
card(x)	The number of nonzero elements in a vector $x \in \mathbf{R}^n$
$\mathcal{N}$	The set of all platforms in a railway network
$\mathcal{A}$	The set of all tracks
$\mathcal{T}$	The set of all trains
$\mathcal{N}^t$	The set of all platforms visited by a train t in chronological order
$\mathcal{A}^t$	The set of all tracks visited by a train t in chronological order
a_i^t	The arrival time of train t at platform i
d_i^t	The departure time of train t from platform i
$[\underline{\tau}_{ij}^t, \overline{\tau}_{ij}^t]$	The trip time window for train t from platform i to platform j
$\mathcal{B}_{ij}$	The set of all train pairs involved in turn-around events on crossing-over (i, j)
$[\underline{\kappa}_{ij}^{tt'}, \overline{\kappa}_{ij}^{tt'}]$	The trip time window for train t on the crossing-over (i, j)
$[\underline{\delta}_i^t, \overline{\delta}_i^t]$	The dwell time window for train t at platform i
χ	The set of all platform pairs situated at the same interchange stations
$\mathcal{C}_{ij}$	The set of connecting train pairs for a platform pair $(i, j) \in \chi$
$[\underline{\chi}_{ij}^{tt'}, \overline{\chi}_{ij}^{tt'}]$	The connection window between train t at platform i and and train t' at platform j
$[0, m]$	The time bound for any event time in the timetable
$\mathcal{H}_{ij}$	The set of train-pairs who move along that track (i, j)
$[\underline{h}_i^{tt'}, \overline{h}_i^{tt'}]$	The headway time window between train t and t' at or from platform i
$[\underline{\tau}_{\mathcal{P}}^t, \overline{\tau}_{\mathcal{P}}^t]$	The total travel time window for train t to traverse its train path
$\tilde{\mathcal{N}}$	The set of all nodes in the constraint graph
$\tilde{\mathcal{A}}$	The set of arcs in the constraint graph
$\tilde{\mathcal{A}}_{trip}$	The set of all arcs associated with trip time constraints
x_i	The arrival or departure time of some train from a platform in the constraint graph
$[l_{ij}, u_{ij}]$	The time window associated with arc (i, j) of the constraint graph
f_{ij}	Energy consumption associated with the trip $(i, j) \in \tilde{\mathcal{A}}_{trip}$
$c_{ij}(x_i - x_j) + b_{ij}$	Affine approximation for f_{ij}
$\left((\bar{a}_i^t, \bar{d}_i^t)_{i \in \mathcal{N}}\right)_{t \in \mathcal{T}}$	Solution to step one optimization model
Ω	The set containing all opposite platform pairs powered by the same electrical substations
$\mathcal{T}_i$	The set of all trains which arrive at, dwell and then depart from platform i
$\vec{t}$	Temporally closest train to the right of train t
$\overset{\leftarrow}{t}$	Temporally closest train to the left of train t
$\tilde{t}$	Temporally closest train to train t
∇_i^t	The relative distance of a_i^t from the regenerative alignment point
$\triangle_j^t$	The relative distance of the consumptive alignment point from d_i^t
$\mathcal{E}$	The set of all synchronization processes between suitable train pairs
$\overset{\rightarrow}{\mathcal{E}}$	A subset of $\mathcal{E}$ containing elements of the form $(i, j, t, \vec{t})$
$\overset{\leftarrow}{\mathcal{E}}$	A subset of $\mathcal{E}$ containing elements of the form $(i, j, t, \overset{\leftarrow}{t})$
env f	Convex envelope of function f

by $(\mathcal{N}, \mathcal{A})$. The set of all trains is denoted by $\mathcal{T}$, where $|\mathcal{T}|$ is fixed. The sets of all platforms and all tracks visited by a train t in chronological order are denoted by $\mathcal{N}^t \subseteq \mathcal{N}$ and $\mathcal{A}^t \subseteq \mathcal{A}$ respectively. The decision variables are the train arrival and departure times, to and from the associated platforms, respectively. Let a_i^t and d_i^t be the arrival time and the departure time of the train $t \in \mathcal{T}$ to and from the platform $i \in \mathcal{N}^t$.

The list of all the symbols used in this paper can be found in (Table 1).

3. Modelling the constraint set

In this section we describe the constraint set for our optimization model. This comprises the feasibility constraints for a railway network of arbitrary topology, and the domain of the decision variables. In every active railway network, the railway management has an operating feasible timetable; we use the sequence of the trains from that timetable. The lower and upper bound of the constraints are integers representing time in seconds.

3.1. Trip time constraint

The trip time constraints play the most important role in train energy consumption and regenerative energy production. These can be of two types as follows.
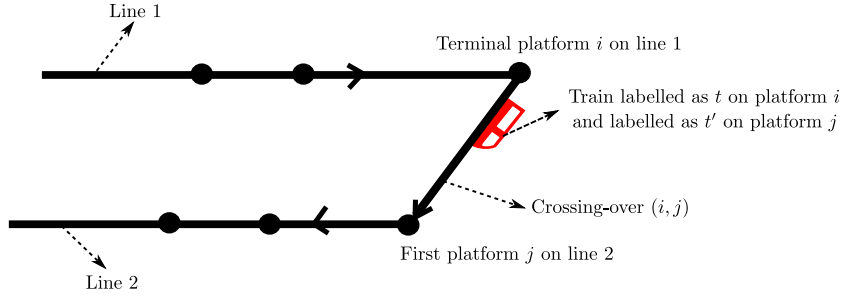
Fig. 3. Trip time constraint associated with a crossing-over.

3.1.1. Trip time constraint associated with a track

Consider the trip of any train $t \in \mathcal{T}$ from platform i to platform j along the track $(i, j) \in \mathcal{A}^t$. The train t departs from platform i at time d_i^t, arrives at platform j at time a_j^t, and it can have a trip time between $\underline{\tau}_{ij}^t$ and $\overline{\tau}_{ij}^t$. The trip time constraint can be written as follows:

$$\forall t \in \mathcal{T}, \quad \forall (i, j) \in \mathcal{A}^t, \quad \underline{\tau}_{ij}^t \leq a_j^t - d_i^t \leq \overline{\tau}_{ij}^t. \tag{1}$$

3.1.2. Trip time constraint associated with a crossing-over

A crossing-over is a special type of directed arc that connects two *train-lines*, where a train-line is a directed path with the set of nodes representing non-opposite platforms and the set of arcs representing non-opposite tracks. If after arriving at the terminal platform of a train-line, a train turns around by traversing the crossing-over and starts travelling through another train-line, then the same physical train is treated and labelled functionally as two different trains by the railway management (Peeters, 2003, page 41). Let φ be the set of all crossing-overs, where turn-around events occur. Consider any crossing-over $(i, j) \in \varphi$, where the platforms i and j are situated on different train-lines. Let $\mathcal{B}_{ij}$ be the set of all train pairs involved in corresponding turn-around events on the crossing-over (i, j). Let $(t, t') \in \mathcal{B}_{ij}$. Train $t \in \mathcal{T}$ turns around at platform i by travelling through the crossing-over (i, j), and beginning from platform j starts traversing a different train-line as train $t' \in \mathcal{T} \setminus \{t\}$. A time window $[\underline{\kappa}_{ij}^{tt'}, \overline{\kappa}_{ij}^{tt'}]$ has to be maintained between the departure of the train from platform i (labelled as train t) and arrival at platform j (labelled as train t'). We can write this constraint as follows:

$$\forall (i, j) \in \varphi, \quad \forall (t, t') \in \mathcal{B}_{ij}, \quad \underline{\kappa}_{ij}^{tt'} \leq a_j^{t'} - d_i^t \leq \overline{\kappa}_{ij}^{tt'}. \tag{2}$$

To clearly illustrate the constraint we consider Fig. 3. Here we have two train lines: line 1 and line 2. The terminal platform on line 1 is platform i and the first platform on line 2 is platform j. The crossing-over from line 1 to line 2 is the arc (i, j). The train shown in the figure is labelled as t on platform i and labelled as train t' on platform j.

3.2. Dwell time constraint

When any train $t \in \mathcal{T}$ arrives at a platform $i \in \mathcal{N}^t$, it dwells there for a certain time interval denoted by $[\underline{\delta}_i^t, \overline{\delta}_i^t]$ so that the passengers can get off and get on the train prior to its departure from platform j. The dwell time constraint can be written as follows:

$$\forall t \in \mathcal{T}, \quad \forall i \in \mathcal{N}^t, \quad \underline{\delta}_i^t \leq d_i^t - a_i^t \leq \overline{\delta}_i^t. \tag{3}$$

Every train $t \in \mathcal{T}$ arrives at the first platform $\mathcal{N}^t(1)$ in its train-path either from the depot or by turning around from some other line, and departs from the final platform $\mathcal{N}^t(|\mathcal{N}^t|)$ in order to either return to the depot or start as a new train on another line by turning around. So, the train t dwells at all platforms in $\mathcal{N}^t$. This is the reason why in Eq. (3) the platform index i is varied over all elements of the set $\mathcal{N}^t$.

3.3. Connection constraint

In many cases, a single train connection might not exist between the origin and the desired destination of a passenger. To circumvent this, connecting trains are often used at interchange stations. Let $\chi \subseteq \mathcal{N} \times \mathcal{N}$ be the set of all platform pairs situated at the same interchange stations, where passengers transfer between trains. Let $\mathcal{C}_{ij}$ be the set of connecting train pairs for a platform pair $(i, j) \in \chi$. For a train pair $(t, t') \in \mathcal{C}_{ij}$, train t is arriving at platform i and train $t' \in \mathcal{T}$ is departing from platform j. A connection time window denoted by $[\underline{\chi}_{ij}^{tt'}, \overline{\chi}_{ij}^{tt'}]$ is maintained between arrival of t and subsequent departure of t', so that passengers can get off from the first train and get on the latter. Let $(i, j) \in \chi$. Then the connection constraint can be written as:

$$\forall (i, j) \in \chi, \quad \forall (t, t') \in \mathcal{C}_{ij}, \quad \underline{\chi}_{ij}^{tt'} \leq d_j^{t'} - a_i^t \leq \overline{\chi}_{ij}^{tt'}. \tag{4}$$

3.4. Headway constraint

In any railway network, a minimum amount of time between the departures and arrivals of consecutive trains on the same track is maintained. This time is called headway time. For maintaining the quality of passenger service, many urban railway system keeps an upper bound between the arrivals and departures of successive trains on the same track, so that passengers do not have to wait too long before the next train comes. Let $(i, j) \in \mathcal{A}$ be the track between two platforms i and j, and $\mathcal{H}_{ij}$ be the set of train-pairs who move along that track successively in order of their departures. Consider $(t, t') \in \mathcal{H}_{ij}$, and let $[\underline{h}_i^{tt'}, \overline{h}_i^{tt'}]$ and $[\underline{h}_j^{tt'}, \overline{h}_j^{tt'}]$ be the time windows that have to be maintained between the departures and arrivals of the trains t and t' from and to the platforms i and j respectively. So, the headway constraint can be written as:

$$\forall (i, j) \in \mathcal{A}, \quad \forall (t, t') \in \mathcal{H}_{ij}, \quad \underline{h}_i^{tt'} \leq d_i^{t'} - d_i^t \leq \overline{h}_i^{tt'} \ \wedge \ \underline{h}_j^{tt'} \leq a_j^{t'} - a_j^t \leq \overline{h}_j^{tt'}. \tag{5}$$

Similarly, headway times have to be maintained between two consecutive trains going through a crossing over. Consider any crossing over $(i, j) \in \varphi$ and two such trains, which leave the terminal platform of a train-line i labelled as t_1 and t_2, traverse the crossing over (i, j), and arrive at platform j of some other train-line labelled as t'_1 and t'_2. The set of all such train quartets $((t_1, t'_1), (t_2, t'_2))$ is represented by $\tilde{\mathcal{H}}_{ij}$. Let $[\underline{h}_i^{t_1 t_2}, \overline{h}_i^{t_1 t_2}]$ be the headway time window between the departures of trains t_1 and t_2 from platform i and $[\underline{h}_j^{t'_1 t'_2}, \overline{h}_j^{t'_1 t'_2}]$ be the headway time window between the arrivals of the trains t'_1 and t'_2 to the platforms j. The associated headway constraints can be written as:

$$\forall (i, j) \in \varphi, \quad \forall ((t_1, t'_1), (t_2, t'_2)) \in \tilde{\mathcal{H}}_{ij}, \quad \underline{h}_i^{t_1 t_2} \leq d_i^{t_2} - d_i^{t_1} \leq \overline{h}_i^{t_1 t_2} \ \wedge \ \underline{h}_j^{t'_1 t'_2} \leq a_j^{t'_2} - a_j^{t'_1} \leq \overline{h}_j^{t'_1 t'_2}. \tag{6}$$

Now we discuss the relation between passenger demand, headway and number of trains. We denote the passenger demand by D, train capacity by c and utilization rate by u. If we denote the number of trains in service per hour by n, then we have

$$D = c \times u \times n$$

(Li and Lo, 2014a). Because the headway time h satisfies the relation $h = \frac{3600}{n}$, we have

$$h = \frac{3600 \times c \times u}{D}. \tag{7}$$

It should be noted that the train capacity c and the utilization rate u are constant parameters. However the passenger demand varies with time. As a result, in the equation above trains will have different headway at different periods.

3.5. Total travel time constraint

The train-path of a train is the directed path containing all platforms and tracks visited by it in chronological order. To maintain the quality of service in the railway network, for every train $t \in \mathcal{T}$, the total travel time to traverse its train-path has to stay within a time window $[\underline{\tau}_{\mathcal{P}}^t, \overline{\tau}_{\mathcal{P}}^t]$. We can write this constraint as follows:

$$\forall t \in \mathcal{T}, \quad \underline{\tau}_{\mathcal{P}}^t \leq a_{\mathcal{N}^t(|\mathcal{N}^t|)}^t - d_{\mathcal{N}^t(1)}^t \leq \overline{\tau}_{\mathcal{P}}^t, \tag{8}$$

where $\mathcal{N}^t(1)$ and $\mathcal{N}^t(|\mathcal{N}^t|)$ are the first and last platform in the train-path of t.

3.6. Domain of the event times

Without any loss of generality, we set the time of the first event of the railway service period, which corresponds to the departure of the first train of the day from some platform, to start at zero second. By setting all trip times and dwell times to their maximum possible values we can obtain an upper bound for the final event of the railway service period, which is the arrival of the last train of the day at some platform, denoted by $m \in \mathbf{Z}_{++}$. So the domain of the decision variables can be expressed by the following equation:

$$\forall t \in \mathcal{T}, \quad \forall i \in \mathcal{N}^t, \quad 0 \leq a_i^t \leq m, 0 \leq d_i^t \leq m. \tag{9}$$

In vector notation the decision variables are denoted by $a = \left((a_i^t)_{i \in \mathcal{N}^t} \right)_{t \in \mathcal{T}}$ and $d = \left((d_i^t)_{i \in \mathcal{N}^t} \right)_{t \in \mathcal{T}}$.

4. First optimization model

In this section we formulate the first optimization model that minimizes the total energy consumed by all trains in the railway network. The organization of this section is as follows. First, in order to keep the proofs less cluttered, we introduce an equivalent constraint graph notation. Then we formulate and justify the first optimization problem. Finally we show that the nonlinear objective of the initial optimization model can be approximated as a linear one by applying least-squares. This results in a linear optimization problem, which has the interesting property that its optimal solution is attained by an integral vector.
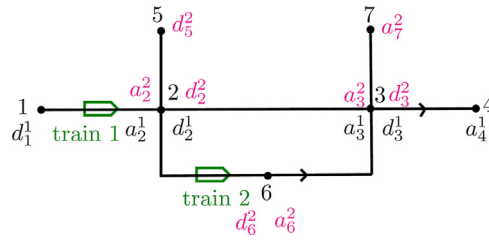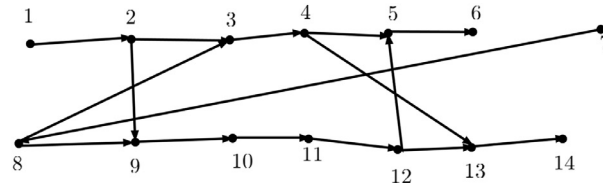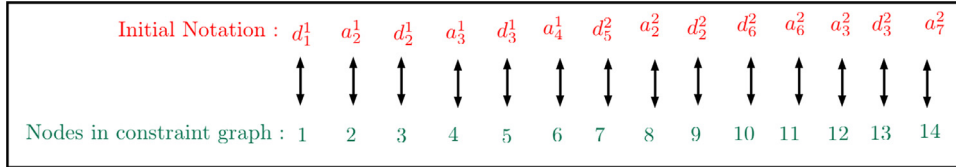
Fig. 4. Example of a very simple railway network.

Fig. 5. The constraint graph for the railway network of Fig. 4.

4.1. Constraint graph notation

Each of the constraints described by Eqs. (1)–(8) is associated with two event times (either arrival or departure time of trains at stations), where one of them precedes another by a time difference dictated by the time window of that constraint. This observation helps us to convert our initial notation into an equivalent constraint graph notation which we describe as follows.

Converting the initial notation into an equivalent constraint graph.

- *Nodes of the constraint graph:* All event times in the original notation are treated as nodes in the constraint graph, the set of those nodes is denoted by $\bar{\mathcal{N}}$ and the value associated with a node $i \in \bar{\mathcal{N}}$ is denoted by x_i, which represents the arrival or departure time of some train from a platform. Consider any two nodes in the constraint graph; if there exists a constraint between the two in the original notation, then in the constraint graph we create a directed arc between them, the start node being the first event and the end node being the later one. The set of arcs thus created in the constraint graph is denoted by $\bar{\mathcal{A}}$. Note that there cannot be more than one arc between two nodes in the constraint graph.
- *Arcs of the constraint graph:* With each arc $(i, j) \in \bar{\mathcal{A}}$ we associate a time window $[l_{ij}, u_{ij}]$ with their values determined from the Eqs. (1)–(8). So, each arc $(i, j) \in \bar{\mathcal{A}}$ corresponds to a constraint of the form $l_{ij} \leq x_j - x_i \leq u_{ij}$. The set of all arcs associated with trip time constraints is expressed by $\bar{\mathcal{A}}_{trip} \subset \bar{\mathcal{A}}$.

Example. Fig. 4 represents a very simple network with 7 stations represented by black dots and 2 trains represented by the directed rectangles. The pointed edge of the symbol indicates the direction. In this network, $\mathcal{T} = \{1, 2\}$ and and the stations are enumerated as $\{1, 2, 3, 4, 5, 6, 7\}$. There are two train lines as shown in the figure. It should be noted that nodes represent stations, not platfrms. Nodes 2 and 3 represent interchange stations, where there are two platforms for both lines on different levels. So, the event times at node 2 and node 3 are associated with different platforms and are differentiated using black and magenta colors. The set of tracks visited by train 1 is $\mathcal{A}^1 = \{(1, 2), (2, 3), (3, 4)\}$, and the set of tracks visited by train 2 is $\mathcal{A}^2 = \{(5, 2), (2, 6), (6, 3), (3, 7)\}$. The set of all tracks is then $\mathcal{A} = \mathcal{A}^1 \cup \mathcal{A}^2$. The event times corresponding to train 1 and train 2 are shown in black and magenta colours respectively in Fig. 4. Applying the conversion process described above we can convert the initial notation in Fig. 4 to the constraint graph shown in Fig. 5.

4.2. Formulation of the first optimization model

A train consumes most of its required electrical energy during the acceleration phase of making a trip from an origin platform to a destination platform. Trip time constraints play the most important role in energy consumption and regenerative energy production of trains. Once the trip time for a trip is fixed, an energy optimal speed profile can be calculated

efficiently by existing software (Vlad and Tatarnikov, 2011), (Howlett and Pudney, 1995, page 285), such as Thales **T**rain **K**inetics, **D**ynamics and **C**ontrol (TKDC) Simulator in our case. The TKDC simulator assumes maximum accelerating - speed holding - coasting - maximum braking strategy for calculation of speed profile. Theoretically this is the optimal speed profile according to the monograph (Howlett and Pudney, 1995). For calculation of the optimal speed profile of a train while making a trip, we refer the interested reader to the highly cited papers (Howlett, 2000; Howlett et al., 2009; Jiaxin and Howlett, 1993; Khmelnitsky, 2000; Liu and Golovitcher, 2003). An excellent state-of-the art review of calculating energy-efficient or energy-optimal speed profile can be found in Albrecht et al. (2015). The key assumptions that we have made in calculating the speed profiles, all of which are well-established in relevant literature (Albrecht et al., 2015), are as follows.

- The acceleration and braking control forces are assumed to be uniformly bounded or bounded by magnitude constraints. These magnitude constraints are assumed to be dependent on the speed of the train and non-increasing.
- The initial speed of the train from the origin platform and final speed at the destination platform are assumed to be zero. The speed is assumed to be strictly positive at every other position.
- Only the force associated with positive acceleration consumes energy.
- The rate of energy dissipation from frictional resistance is assumed to be a quadratic function of the form $a_0 + a_1 v + a_2 v^2$ (also known as the *Davis formula* (Davis, 1926)), where v stands for speed of the train and a_0, a_1, a_2 are non-negative physical constants. These constants can be determined approximately in practice by measuring the difference between the applied tractive force and the net tractive force.
- We have assumed the position of the train to be an independent variable and speed of the train to be a dependent variable. This assumption appears all the major contributions. This assumption appears all the major contributions. A notable exception is Khmelnitsky (2000), which considers kinetic energy and time as the dependent variables and position as the independent variable.

The electrical power consumption and regeneration of a train on a track is determined by its speed profile, so the optimal speed profile also gives the power versus time graph (*power graph* in short) for that trip. However, in the total railway service period there are many active trains, whose movements are coupled by the associated constraints. So, finding the energy-minimal trip time for a single trip in an isolated manner can result in a infeasible timetable. Consider an arc $(i, j) \in \bar{A}_{trip}$ in the constraint graph, associated with some trip time constraint. Let us denote the energy consumption function for that trip $f_{ij} : \mathbf{R}_{++} \to \mathbf{R}_{++}$ with argument $(x_j - x_i)$. The first optimization problem with the objective to minimize the total energy consumption of the trains can be written as:

$$
\begin{aligned}
\text{minimize} \quad & \sum_{(i,j) \in \bar{A}_{trip}} f_{ij}(x_j - x_i) \\
\text{subject to} \quad & l_{ij} \le x_j - x_i \le u_{ij}, \quad \forall (i, j) \in \bar{A} \\
& 0 \le x_i \le m, \quad \forall i \in \bar{\mathcal{N}},
\end{aligned}
\tag{10}
$$

where the decision vector is $(x_i)_{i \in \bar{N}} \in \mathbf{R}^{|\bar{N}|}$.

The exact analytical form of every component of the objective function, *i.e.*, $f_{ij}(x_j - x_i)$ for $(i, j) \in \bar{A}_{trip}$ is not known and may be intractable (Howlett et al., 2009). However, irrespective of the exact analytical form, the energy function can be shown to be monotonically decreasing in trip time, *i.e.*, it is *non-increasing* with the increase in trip time, if the optimal speed profile is followed (Milroy, 1980). Even when a train is manually driven with possibly suboptimal driving strategies, the average energy consumption of the train is found empirically to be monotonically decreasing in the trip time (Peña-Alcaraz et al., 2012b).

Also, the energy function is relatively easy to measure in practice (Howlett and Pudney, 1995, Section 1.5). For any $(i, j) \in \bar{A}_{trip}$, we denote the measured trip times $(x_j^{(1)} - x_i^{(1)}), \ldots, (x_j^{(p)} - x_i^{(p)})$ and the corresponding energy consumption data $f_{ij}^{(1)}, \ldots, f_{ij}^{(p)}$.

In any subway system, the amount by which the trip time is allowed to vary in Eqs. (1) and (2) is typically on the order of seconds (Liebchen, 2007), which motivates us to make the following assumption.

Assumption 1. The amount by which the trip time is allowed to vary is on the order of seconds, i.e., for any the trip time window is on the order of seconds.

The monotonically decreasing nature of the energy function together with Assumption 1 allows us to approximate the energy function $f_{ij}(x_j - x_i)$ as an affine function. Recall that in practice, we can measure the energy $f_{ij}^{(1)}, \ldots, f_{ij}^{(p)}$ and associated trip times $(x_j^{(1)} - x_i^{(1)}), \ldots, (x_j^{(p)} - x_i^{(p)})$, which is obtainable easily with present technology (Howlett and Pudney, 1995, Section 1.5).

Now we want to formulate an optimization problem which will provide us with the best possible affine approximation of the energy function $f_{ij}(x_j - x_i)$. We do so by applying least-squares and fit a straight line through measured energy versus trip time data. We seek an affine function $c_{ij}(x_j - x_i) + b_{ij} = (x_j - x_i, 1)^T (c_{ij}, b_{ij})$ where we want to determine c_{ij} and b_{ij}.

The affine function approximates the measured energy in the least-squares sense as follows:

$$
\begin{aligned}
(c_{ij}, b_{ij}) &= \underset{(\tilde{c}_{ij}, \tilde{b}_{ij})}{\operatorname{argmin}} \sum_{k=1}^{p} \left(\tilde{c}_{ij}(x_j^{(k)} - x_i^{(k)}) + \tilde{b}_{ij} - f_{ij}^{(k)} \right)^2 \\
&= \underset{(\tilde{c}_{ij}, \tilde{b}_{ij})}{\operatorname{argmin}} \left\| \begin{bmatrix} (x_j^{(1)} - x_i^{(1)}, 1)^T \\ \vdots \\ (x_j^{(p)} - x_i^{(p)}, 1)^T \end{bmatrix} \begin{bmatrix} \tilde{c}_{ij} \\ \tilde{b}_{ij} \end{bmatrix} - \begin{bmatrix} f_{ij}^{(1)} \\ \vdots \\ f_{ij}^{(p)} \end{bmatrix} \right\|_2^2
\end{aligned}
\tag{11}
$$

The problem above is an unconstrained optimization problem with convex quadratic differentiable objective. So it can be solved by taking the gradient with respect to $(\tilde{c}_{ij}, \tilde{b}_{ij})$, setting the result equal to zero vector and then solving for $(\tilde{c}_{ij}, \tilde{b}_{ij})$. This yields the following closed form solution:

$$
\begin{bmatrix} c_{ij} \\ b_{ij} \end{bmatrix} = \left(\begin{bmatrix} (x_j^{(1)} - x_i^{(1)}, 1)^T \\ \vdots \\ (x_j^{(p)} - x_i^{(p)}, 1)^T \end{bmatrix}^T \begin{bmatrix} (x_j^{(1)} - x_i^{(1)}, 1)^T \\ \vdots \\ (x_j^{(p)} - x_i^{(p)}, 1)^T \end{bmatrix} \right)^{-1} \begin{bmatrix} (x_j^{(1)} - x_i^{(1)}, 1)^T \\ \vdots \\ (x_j^{(p)} - x_i^{(p)}, 1)^T \end{bmatrix}^T \begin{bmatrix} f_{ij}^{(1)} \\ \vdots \\ f_{ij}^{(p)} \end{bmatrix}
\tag{12}
$$

Using Eq. (12), we can approximate the nonlinear objective of the optimization problem (10) as an affine one: $\sum_{(i,j) \in \bar{A}_{trip}} c_{ij}(x_i - x_j) + b_{ij}$. A measurement of the quality of such fittings is given by the *coefficient of determination*, which can vary between 0 to 1, with 0 being the worst and 1 being the best (Kapadia et al., 2005, page 518). In our numerical studies the mean coefficient of determination of the energy fittings over all the different trips of all the trains is found to be 0.9483 with a standard deviation of 0.05, which justifies our approach. We can also discard the b_{ij}s from the objective, as it has no impact on the minimizer. Thus we arrive at the following linear optimization problem to minimize the total energy consumption of the trains:

$$
\begin{aligned}
\text{minimize} \quad & \sum_{(i,j) \in \bar{A}_{trip}} c_{ij}(x_j - x_i) \\
\text{subject to} \quad & l_{ij} \leq x_j - x_i \leq u_{ij}, \quad \forall (i,j) \in \bar{A} \\
& 0 \leq x_i \leq m, \quad \forall i \in \bar{N}.
\end{aligned}
\tag{13}
$$

Note that, we have not used the same cost-time curve for all the trips. Each of the constituent parts $c_{ij}(x_j - x_i)$ of the objective function $\sum_{(i,j) \in \bar{A}_{trip}} c_{ij}(x_j - x_i)$ in Problem (12) represents approximated affine function for each of the trips considered in the optimization problem. If optimal speed profiles for the trips are available to the railway management, from the first optimization model the optimal trip times for those optimal speed profiles can be found. If available speed profiles are suboptimal, then the first optimization model would still produce an energy-efficient timetable with best trip times subject to the available speed profiles.

An important property of this optimization model is that the polyhedron associated with optimization problem has only integer vertices, so the optimal value is attained by an integral vector. A necessary and sufficient condition of integrality of the vertices of a polyhedron is given by the following theorem (Schrijver, 1998, page 269, Theorem 19.3), which we will use to prove the subsequent proposition.

Theorem 1. *Let A be a matrix with entries $0, +1,$ or -1. For all integral vectors a, b, c, d the polyhedron $\{x \in \mathbf{R}^n | c \preceq x \preceq d, a \preceq Ax \preceq b\}$ has only integral vertices if and only if for each nonempty collection of columns of A, denoted by C, there exist two subsets , C_1 and C_2 such that $C_1 \cup C_2 = C, C_1 \cap C_2 = \emptyset$, and the sum of the columns in C_1 minus the sum of the columns in C_2 is a vector with entries 0, 1 and -1.*

Proposition 1. *The optimization problem (13) has an integral optimal solution.*

Proof. We write the problem (13) in vector form. We construct a cost vector c, such that a component of that vector is c_{ij} if it is associated with a trip time constraint in the original notation, and zero otherwise. Construct integral vectors $l = (l_{ij})_{(i,j) \in \bar{A}}$, $u = (u_{ij})_{(i,j) \in \bar{A}}$ and matrix $A \in \{-1, 0, 1\}^{|\bar{A}| \times |\bar{N}|}$ such that the (k, i)th entry of the matrix A, denoted by a_{ki}, is associated with the kth hyperarc and ith node of the constraint graph as follows:

$$
a_{ki} = \begin{cases} 1 & \text{if node } i \text{ is the end node of hyperarc k,} \\ -1 & \text{if node } i \text{ is the start node of hyperarc k,} \\ 0 & \text{otherwise.} \end{cases}
$$

So, the vector form of the optimization problem (13) is:

$$
\begin{aligned}
\text{minimize} \quad & c^T x \\
\text{subject to} \quad & l \preceq Ax \preceq u, \\
& 0 \preceq x \preceq m\mathbf{1}.
\end{aligned}
\tag{14}
$$

Consider any nonempty collection of columns of A denoted by C. Take $C_1 = C$ and $C_2 = \emptyset$. Then the sum of the columns in C_1 minus the sum of the columns in C_2 will be a vector with entries 0, 1 and -1, because in A there cannot exist more than one row corresponding to an arc between two nodes of the constraint graph and each such row has exactly two nonzero entries, a $+1$ and a -1. So, by Theorem 1 the polyhedron $\{x \in \mathbf{R}^{|\mathcal{N}|} : l \preceq Ax \preceq u, 0 \preceq x \preceq m\mathbf{1}\}$ has only integral vertices and optimizing the linear objective in problem (14) over this polyhedron will result in an integral solution. $\square$

After solving the linear programming problem (13), we obtain an integral timetable, which we will call the energy minimizing timetable (**EMT**). We denote the optimal decision vector of this timetable by $\bar{x}$ in the constraint graph notation and $\left((\bar{a}_i^t, \bar{d}_i^t)_{i \in \mathcal{N}} \right)_{t \in \mathcal{T}}$ in the original notation.

5. Second optimization model

In this section we modify the trip time constraints such that the total energy consumption of the final timetable is kept at the same minimum as the EMT. Then, we describe our optimization strategy aimed to maximize the utilization of regenerative energy of braking trains, and we present the second optimization model.

5.1. Keeping the total energy consumption at minimum

In any feasible timetable, if the trip times are kept to be the same as the ones obtained from the EMT, then the energy optimal speed profiles for all trains will be the same. As a result, the energy consumption associated with that timetable will remain at the same minimum as found in the EMT. So, in the second optimization problem, instead of using the trip time constraint, for every trip we fix the trip time to the value in the EMT, *i.e.*,

$$\forall t \in \mathcal{T}, \quad \forall (i, j) \in \mathcal{A}^t, \quad a_j^t - d_i^t = \bar{a}_j^t - \bar{d}_i^t, \tag{15}$$

and

$$\forall (i, j) \in \varphi, \quad \forall (t, t') \in \mathcal{B}_{ij}, \quad a_j^{t'} - d_i^t = \bar{a}_j^{t'} - \bar{d}_i^t. \tag{16}$$

For all other constraints, bounds are allowed to vary as described by Eqs. (3)–(8). As a consequence of fixing all trip times, the power graph of every trip made by any train becomes known to us, since it depends on the corresponding optimal speed profile calculated in real-time by existing software (Vlad and Tatarnikov, 2011), (Howlett and Pudney, 1995, page 285).

5.2. Maximizing the utilization of regenerative energy of braking trains

In this subsection we describe our strategy to maximize the utilization of the regenerative energy produced by the braking trains. Strategies based on transfer of regenerative braking energy back to the electrical grid requires specialized technology such as reversible electrical substations (González-Gil et al., 2013). A strategy based on storing is not feasible with present technology, because storage options such as super-capacitors, fly-wheels, *e.t.c.*, have drastic discharge rates besides being too expensive (Avinash Balakrishnan, 2014, page 66), (Droste-Franke et al., 2012, page 92). A better strategy that can be used with existing technology (Ciccarelli et al., 2014) is to transfer the regenerative energy of a braking train to a nearby and simultaneously accelerating train, if both of them operate under the same electrical substation. We call such pairs of trains *suitable train pairs*. So our objective is to maximize the total overlapped area between the graphs of power consumption and regeneration of all suitable train pairs. To model this mathematically, we are faced with the following tasks: *i)* define suitable train pairs, *ii)* provide a tractable description of the overlapped area between power graphs of such a pair. We describe them as follows.

5.2.1. Defining suitable train pairs

We consider platform pairs who are opposite to each other and are powered by the same electrical substations. Thus, the transmission loss in transferring electrical energy between them is negligible. In our work we The set containing all such platform pairs is denoted by Ω. Consider any such platform pair $(i, j) \in \Omega$, and let $\mathcal{T}_i \subseteq \mathcal{T}$ be the set of all trains which arrive at, dwell and then depart from platform i. Suppose, $t \in \mathcal{T}_i$. Now, we are interested in finding another train $\tilde{t}$ on platform j, *i.e.*, $\tilde{t} \in \mathcal{T}_j$, which along with t would form a suitable pair for the transfer of regenerative braking energy. To achieve this, we use the EMT. Among all trains going through platform j, the one which is temporally closest to t in the energy-minimizing timetable is be the best candidate to form a pair with t. The temporal proximity can be of two types with respect to t, which results in the following definitions.

Definition 1. Consider any $(i, j) \in \Omega$. For every train $t \in \mathcal{T}_i$, the train $\overrightarrow{t} \in \mathcal{T}_j$ is called the **temporally closest train to the right of t** if

$$\overrightarrow{t} = \underset{t' \in \{x \in \mathcal{T}_j : 0 \leq \frac{\bar{a}_j^x + \bar{d}_j^x}{2} - \frac{\bar{a}_i^t + \bar{d}_i^t}{2} \leq r\}}{\operatorname{argmin}} \left\{ \left| \frac{\bar{a}_i^t + \bar{d}_i^t}{2} - \frac{\bar{a}_j^{t'} + \bar{d}_j^{t'}}{2} \right| \right\}, \tag{17}$$

where r is an empirical parameter determined by the timetable designer and is much smaller than the time horizon of the entire timetable.

Definition 2. Consider any $(i, j) \in \Omega$. For every train $t \in \mathcal{T}_i$, the train $\overleftarrow{t} \in \mathcal{T}_j$ is called the **temporally closest train to the left of t** if

$$\overleftarrow{t} = \underset{t' \in \{x \in \mathcal{T}_j : 0 < \frac{\bar{a}_i^t + \bar{d}_i^t}{2} - \frac{\bar{a}_j^x + \bar{d}_j^x}{2} \leq r\}}{\operatorname{argmin}} \left\{ \left| \frac{\bar{a}_i^t + \bar{d}_i^t}{2} - \frac{\bar{a}_j^{t'} + \bar{d}_j^{t'}}{2} \right| \right\}. \tag{18}$$

Definition 3. Consider any $(i, j) \in \Omega$. For every train $t \in \mathcal{T}_i$, the train $\tilde{t} \in \mathcal{T}_j$ is called the **temporally closest train to t** if

$$\tilde{t} = \underset{t' \in \{\overrightarrow{t}, \overleftarrow{t}\}}{\operatorname{argmin}} \left\{ \left| \frac{\bar{a}_i^t + \bar{d}_i^t}{2} - \frac{\bar{a}_j^{t'} + \bar{d}_j^{t'}}{2} \right| \right\}. \tag{19}$$

If both $\overrightarrow{t}$ and $\overleftarrow{t}$ are temporally equidistant from t, we pick one of them arbitrarily.

Any synchronization process between a suitable train pair (SPSTP) can be described by specifying the corresponding i, j, t and $\tilde{t}$ by using the definitions above. We construct a set of all SPSTPs, which we denote by $\mathcal{E}$. Each element of this set is a tuple of the form $(i, j, t, \tilde{t})$. Because $\tilde{t}$ is unique for any t in each element of $\mathcal{E}$, we can partition $\mathcal{E}$ into two sets denoted by $\overrightarrow{\mathcal{E}}$ and $\overleftarrow{\mathcal{E}}$ containing elements of the form $(i, j, t, \overrightarrow{t})$ and $(i, j, t, \overleftarrow{t})$ respectively.

Remark. Now we compare our design choice to that of (Yang et al., 2013), which considers two additional scenarios: two trains 1) on two consecutive platforms on the same track, or 2) on the same platform on same track. In the first case, there will of course be a significant distance between the two trains, and in the second case, we need to maintain at least the safety distance between the two trains irrespective of how small the headway is. First, to transfer the regenerative energy to the accelerating trains, we would need either supercapacitors, or fly-wheels, both of which have drastic discharge rates (Avinash Balakrishnan, 2014, page 66), (Droste-Franke et al., 2012, page 92). Additionally, if we consider resistive transmission loss, in practice there would be very little or no energy transfer due to the power loss along the line. Note that in (Yang et al., 2013) this issue would not arise, as they have assumed no transmission loss.

5.2.2. Description of the overlapped area between power graphs

The power graph during accelerating and braking is highly nonlinear in nature with no analytic form, as shown in Fig. 6. So, maximizing the exact overlapped area will lead to an intractable optimization problem. However, the existence of dominant peaks with sharp falls allows us to apply a robust lumping method such as $\frac{1}{e}$ heuristic (Mahajan, 2010, page 33–34) to approximate the power graphs as rectangles. The $\frac{1}{e}$ heuristic is applied as follows (see Fig. 6). The height of the rectangle is the maximum power, and the width is the interval with extreme points corresponding to power dropped at $1/e$ of the maximum. For the sharp drop from the peak, such rectangles are very robust approximations to the original power graph containing the most concentrated part of the energy, *e.g.*, if the drop were exponential, then the energy contained by the rectangle would have been exactly equal to that of the original curve (Mahajan, 2010, page 33–34). After converting both the power graphs to rectangles, maximizing the overlapped area under those rectangles is equivalent to aligning the midpoint of the width of the rectangles; we call such a midpoint **regenerative or consumptive alignment point**. These alignment points act as virtual peaks of the approximated power graphs. As shown in Fig. 6, for a train t in its braking phase prior to its arrival at platform i, the relative distance of a_i^t from the regenerative alignment point is denoted by $\triangledown_i^t$, while during acceleration the relative distance of the consumptive alignment point from d_i^t is denoted by $\triangle_j^t$. Note that both relative distances are known parameters for the current optimization problem.

5.3. Second optimization model

Consider an element $(i, j, t, \overrightarrow{t}) \in \overrightarrow{\mathcal{E}}$. To ensure the transfer of maximum possible regenerative energy from the braking train $\overrightarrow{t}$ to the accelerating train t, we aim to align both their alignment points such that $d_i^t + \triangle_i^t = a_j^{\overrightarrow{t}} - \triangledown_j^{\overrightarrow{t}}$, or keep them as close as possible otherwise. Similarly, for any $(i, j, t, \overleftarrow{t}) \in \overleftarrow{\mathcal{E}}$, our objective is $d_j^{\overleftarrow{t}} + \triangle_j^{\overleftarrow{t}} = a_i^t - \triangledown_i^t$, or as close as possible. Let a decision vector y be defined as

$$y = \left(\left(d_i^t + \triangle_i^t - a_j^{\overrightarrow{t}} + \triangledown_j^{\overrightarrow{t}} \right)_{(i,j,t,\overrightarrow{t}) \in \overrightarrow{\mathcal{E}}}, \left(d_j^{\overleftarrow{t}} + \triangle_j^{\overleftarrow{t}} - a_i^t + \triangledown_i^t \right)_{(i,j,t,\overleftarrow{t}) \in \overleftarrow{\mathcal{E}}} \right). \tag{20}$$

Then our goal comprises of two parts: 1) maximize the number of zero components of y which corresponds to minimizing **card**(y), and 2) keep the nonzero components as close to zero as possible which corresponds to minimizing the ℓ_1 norm of
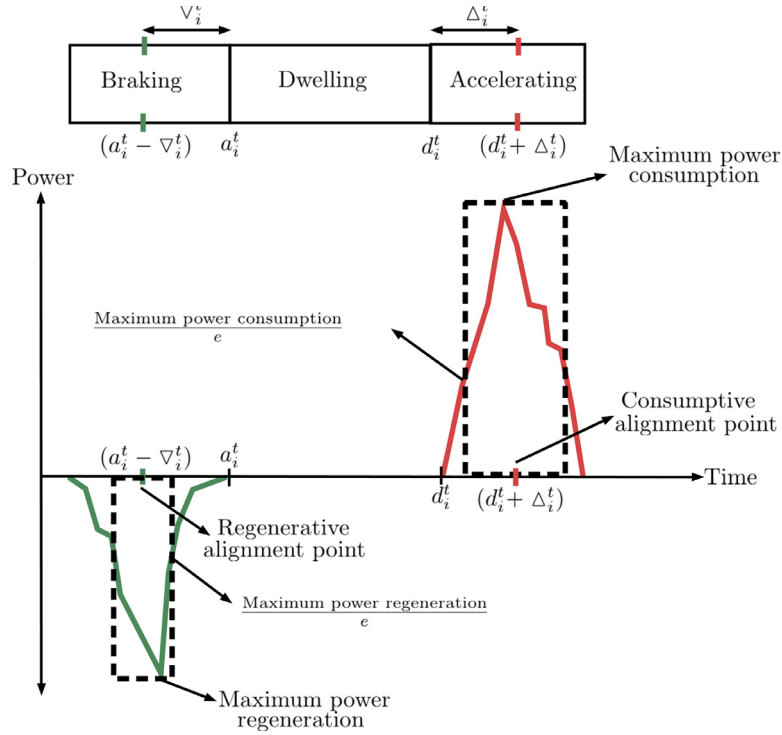
Fig. 6. Applying $\frac{1}{e}$ heuristic to power graphs.

y, $\|y\|_1$. Combining these two we can write the exact optimization problem as follows:

$$\begin{aligned}
\text{minimize} \quad & \mathbf{card}(y) + \gamma \|y\|_1 \\
\text{subject to} \quad & \\
& \text{Eq. (3)–(8),(15),(16),(20),} \\
& 0 \leq a_i^t \leq m, 0 \leq d_i^t \leq m, \quad \forall i \in \mathcal{N}^t, \quad \forall t \in \mathcal{T},
\end{aligned} \tag{21}$$

where γ is a positive weight, and decision variables are a, d and y. The objective function is nonconvex as shown next. Take the convex combination of the vectors $2e_1/\gamma$ and 0 with convex coefficients $1/2$. Then,

$$\mathbf{card}\left(\frac{e_1}{\gamma}\right) + \gamma \left\|\frac{e_1}{\gamma}\right\|_1 = 2 > \frac{1}{2}\left(\mathbf{card}\left(\frac{2e_1}{\gamma}\right) + \gamma \left\|\frac{2e_1}{\gamma}\right\|_1\right) + \frac{1}{2}\left(\mathbf{card}\,(0) + \gamma\|0\|_1\right) = 1.5,$$

and thus violates definition of a convex function. As a result, problem (21) is a nonconvex problem. Note that if we remove the cardinality part from the objective, then it reduces to a convex optimization problem because the constraints are affine and the objective is the ℓ_1 norm of an affine transformation of the decision variables (Boyd and Vandenberghe, 2009, pages 72, 79, 136–137). Such problems are often called convex-cardinality problem and are of $\mathcal{NP}$-hard computational complexity in general (Calafiore and El Ghaoui, 2014). An effective yet tractable numerical scheme to achieve a low-cardinality solution in a convex-cardinality problem is the ℓ_1 norm heuristic, where $\mathbf{card}(y)$ is replaced by $\|y\|_1$, thus converting problem (21) into a convex optimization problem. This is described by problem (22) below. The ℓ_1 norm heuristic is supported by extensive numerical evidence with successful applications to many fields, *e.g.*, robust estimation in statistics, support vector machine in machine learning, total variation reconstruction in signal processing, compressed sensing *etc*. In the next section we show that in our problem too, the ℓ_1 norm heuristic produces excellent results. Intuitively, the ℓ_1 norm heuristic works well, because it encourages sparsity in its arguments by incentivizing exact alignment between regenerative alignment points with the associated consumptive ones (Boyd and Vandenberghe, 2009, pages 300–301). We provide a theoretical justification for the use of ℓ_1 norm in our case as follows.

Proposition 2. *The convex optimization problem described by*

$$\begin{aligned}
\text{minimize} \quad & \|y\|_1 \\
\text{subject to} \quad & \\
& \text{Eq. (3)-(8),(15),(16),(20),} \\
& 0 \leq a_i^t \leq m, 0 \leq d_i^t \leq m, \quad \forall i \in \mathcal{N}^t, \quad \forall t \in \mathcal{T},
\end{aligned} \tag{22}$$

is the best convex approximation of the nonconvex problem (21) from below.

Proof. Both problems (22) and (21) have the same constraint set, so we need to focus on the objective only. The best convex approximation of a nonconvex function $f: C \to \mathbf{R}$ (where C is any set) from below is given by its convex envelope **env** f on C. The function **env** f is the largest convex function that is an under estimator of f on C, i.e.,

$$\mathbf{env}\, f = \sup\{\tilde{f}: C \to \mathbf{R} \mid \tilde{f} \text{ is convex and } \tilde{f} \le f\},$$

where sup stands for the supremum, , the least upper bound of the set. The definition implies, **epi env** $f = \mathbf{conv}\,\mathbf{epi}\, f$.

From Eq. (20) we see that y is an affine transformation of a and d, and from the last constraints of problem (21) we see that both a and d are upper bounded by m, i.e., $\|a\|_\infty \le m$ and $\|d\|_\infty \le m$. So there exists a positive number P such that $\|y\|_\infty \le P$. As the domain of y is bounded in an ℓ_∞ ball with radius P, $\mathbf{env}\,\mathbf{card}(y) = \frac{1}{P}\|y\|_1$ (Calafiore and El Ghaoui, 2014, page 321). So, the best convex approximation of the objective from below is $\frac{1}{P}\|y\|_1 + \gamma \|y\|_1 = (\frac{1}{P} + \gamma)\|y\|_1$. As the coefficient $(\frac{1}{P} + \gamma)$ is a constant for a particular optimization problem, it can be omitted, and thus we arrive at the claim. □

Using the epigraph approach (Boyd and Vandenberghe, 2009, pages 143–144), we can transform the convex problem (22) into a linear program as follows. For each $(i, j, t, \vec{t}) \in \vec{\mathcal{E}}$ and each $(i, j, t, \overleftarrow{t}) \in \overleftarrow{\mathcal{E}}$, we introduce new decision variables $\theta_{ij}^{t\vec{t}}$ and $\theta_{ij}^{t\overleftarrow{t}}$ respectively, such that $\theta_{ij}^{t\vec{t}} \ge |d_i^t + \triangle_i^t - a_j^{\vec{t}} + \triangledown_j^{\vec{t}}|$ and $\theta_{ij}^{t\overleftarrow{t}} \ge |d_j^{\overleftarrow{t}} + \triangle_j^{\overleftarrow{t}} - a_i^t + \triangledown_i^t|$. Then, the convex optimization problem can be converted into the following linear problem:

$$
\begin{aligned}
\text{minimize} \quad & \sum_{(i,j,t,\vec{t})\in\vec{\mathcal{E}}} \theta_{ij}^{t\vec{t}} + \sum_{(i,j,t,\overleftarrow{t})\in\overleftarrow{\mathcal{E}}} \theta_{ij}^{t\overleftarrow{t}} \\
\text{subject to} \quad & \\
& \theta_{ij}^{t\vec{t}} \ge d_i^t + \triangle_i^t - a_j^{\vec{t}} + \triangledown_j^{\vec{t}}, \qquad \forall (i,j,t,\vec{t}) \in \vec{\mathcal{E}} \\
& \theta_{ij}^{t\vec{t}} \ge -d_i^t - \triangle_i^t + a_j^{\vec{t}} - \triangledown_j^{\vec{t}}, \qquad \forall (i,j,t,\vec{t}) \in \vec{\mathcal{E}} \\
& \theta_{ij}^{t\overleftarrow{t}} \ge d_j^{\overleftarrow{t}} + \triangle_j^{\overleftarrow{t}} - a_i^t + \triangledown_i^t, \qquad \forall (i,j,t,\overleftarrow{t}) \in \overleftarrow{\mathcal{E}} \\
& \theta_{ij}^{t\overleftarrow{t}} \ge -d_j^{\overleftarrow{t}} - \triangle_j^{\overleftarrow{t}} + a_i^t - \triangledown_i^t, \qquad (i,j,t,\overleftarrow{t}) \in \overleftarrow{\mathcal{E}} \\
& \text{Eq. (3)-(8),(15),(16),} \\
& 0 \le a_i^t \le m, 0 \le d_i^t \le m \qquad \forall t \in \mathcal{T}, \quad \forall i \in \mathcal{N}^t,
\end{aligned}
\tag{23}
$$

where the decision variables are $a_i^t, d_i^t, \theta_{ij}^{t\vec{t}}$ and $\theta_{ij}^{t\overleftarrow{t}}$.

6. Limitations of the optimization model

In this section, we discuss the limitations of our model as follows.

- We have assumed that the amount by which the trip time is allowed to vary is on the order of seconds (Assumption 1). Though this is true for most of the subway systems, there are exceptions where this assumption may not hold. For example, when a trip between two cities is considered (especially involving different countries), the trip is on the order of hours with the acceptable trip time bound often being on the order of 5–10 min and even more in some cases. In such a scenario, an affine approximation of the energy with respect to trip time would not be very efficient any more, and our model would not be suitable for such a case.
- In Section 5 we have have applied two different heuristics to arrive at a convex optimization problem. At first we have used $\frac{1}{e}$ heuristic to come up with a tractable description of the overlapped area between power graphs, and then we have used the ℓ_1 norm heuristic to approximate a nonconvex objective function with its convex envelope. So, it is quite likely that the timetable obtained by solving the convex optimization problem (Problem 23) would have a worse objective value compared to the original intractable optimization problem. For this reason our model is energy-efficient, but not necessarily energy-optimal.
- The model does not directly address the case of significant delay. However, we have considered two indirect ways of dealing with it in practice.
  - In any automatic train supervision system, which has the responsibility of implementing the timetable, dwell and velocity regulation are performed to maintain trains on their proper time. If there is a deviation from the optimal timetable because of some delay, the ATS performs regulation to move delayed trains back to the planned optimal timetable timetable. Thus the system will typically return to a normal state in less than half an hour after a delay of one minute.
  - Another way is incorporating the change in the system (due to the delay) as an input data and solving a new but shorter optimization problem with a time horizon of 1–2 h which can be done in real time using our model. While the shorter model is being implemented we solve the larger optimization problem spanning the rest of the day.

7. Numerical study

In this section we apply our model to different problem instances spanning full service period of one day to service PES2-SFM2 of line 8 of Shanghai Metro network. Shanghai Metro is the world's largest rapid transit system by route length,
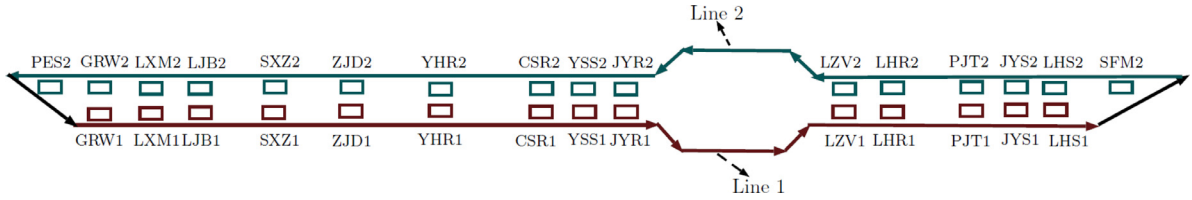
Fig. 7. Railway network considered for numerical study.

second largest by number of stations(after Beijing), and third oldest rapid transit system in mainland China. Line 8, opened on December of 2007, is one of the 14 lines of the Shanghai Metro Network. It passes by some of Shanghai's densest neighborhoods, and has a daily ridership of approximately 1.08 million (2014 peak). This line is 37.4 km long with 28 stations in operation (Group, 2015). The service PES2-SFM2 of line 8 of the Shanghai Metro network is shown in Fig. 7. There are two lines in this network: Line 1 and Line 2. There are fourteen stations in the network denoted by all capitalized words in the figure. Each station has two platforms each on different train lines, *e.g.*, LXM is station that has two opposite platforms: LXM1 and LXM2 on Line 1 and Line 2 respectively. The platforms are denoted by rectangles. The platforms indicated by PES2 and SFM2 are the turn-around points on Line 2, with the crossing-overs being PES2-GRW1 and LHS1-SFM2. The number of trains, headway times, speed of the involved trains, the grades of the tracks and nature of the energy profile of the associated acceleration and braking phases are different for different instances.

Now we provide some relevant information regarding the railway network in consideration. The line is 37 km long. The average distance between two stations in this network is 1.4 km, with the minimum distance being 738 m (between YHR and ZJD) and maximum distance being 2.6 km (between PJT and LHR). The slope of the track is in $[-2.00453°, 2.00453°]$. The maximum allowable acceleration of a train is 1.04 m/s^2 at accelerating phase. The maximum allowable deceleration rate of a train during coasting phase is -0.2 m/s^2. The maximum allowable deceleration of a train during braking phase is -0.8 m/s^2. The conversion factor from electricity to kinetic energy is 0.9, and the conversion factor from kinetic to regenerative braking energy is 0.76. The transmission loss factor of regenerative electricity is 0.1. The mass of the train is in [229370, 361520] kg, with the average mass being 295445 kg.

The data on speed limit is described by Table 3 in Appendix. The speed limit data are based on grade and curvature of the tracks, and operational constraints present in the system. For the railway network, the tracks have piece-wise speed limits for trains, *i.e.,* each track (except CSR2-YHR2) is divided into multiple segments, where each segment has a constant speed limit. The track CSR2-YHR2 has only one segment (itself) with a speed limit of 60 km/h. Table 3 is provided to us by Thales Canada Inc.

The numerical study was executed on a Intel Core i7-46400 CPU with 8 GB RAM running Windows 8.1 Pro- operating system. For modelling the problem, we have used JuMP - an open source algebraic modelling language embedded in programming language Julia (Lubin and Dunning, 2015). Within our JuMP code we have called academic version of Gurobi Optimizer 6.0 as the solver. We have implemented an interior point algorithm because of the underlying sparsity in the data structure. As mentioned before, a measure of the quality of affine fittings using least-squares approach is given by the *coefficient of determination*, which can vary between 0 to 1, with 0 being the worst and 1 being the best (Mendenhall et al., 2009, page 518). In our numerical study, the average coefficient of determination of the affine fittings for energy versus trip times over all different trips and all trains is found to be 0.9483 with a standard deviation of 0.05, which justifies our approach.

The duration of the timetables is eighteen hours which is the full service period of the railway network. We have considered eleven different instances with varying average headway times and number of trains. The number of trains increases as the average headway time decreases, where the relation between them can be determined from Eq. 7. The results of the numerical study are shown in Table 2.

We can see that, in all of the cases our model has found the optimal timetables very quickly, the largest runtime being 12.58s. To the best of our knowledge, this model is the only one to calculate energy-efficient railway timetable spanning an entire day, the next largest being 6 hours only (Das Gupta et al., 2015) with a much larger computation time for smaller sized problems. After we get the final timetable, we calculate the total *effective energy consumption* by all trains involved in SPSTPs and compare it with the original timetables. The effective energy consumption of a train during a trip is defined as the difference between the total energy required to make a trip and the amount of energy that is being supplied by a braking train during synchronization process. So, the effective energy consumption is the energy that will be consumed from the electrical substations.

Now we briefly point out how the total energy consumption is calculated theoretically. Consider the trip of any train t of mass m_t from one platform to the next one. Assume the trip time to make the trip is *T*. At time instance τ, the acceleration, speed, position, and resistive acceleration is denoted by $u_t(\tau)$, $v_t(\tau)$, $s_t(\tau)$ and $-r(v_t(\tau))$, respectively. The resistive acceleration is given by the *Davis formula* (Davis, 1926)

$$r(v_t(\tau)) = a_0 + a_1 v_t(\tau) + a_2 v_t^2(\tau),$$

Table 2
Results of the numerical study performed to line 8 of Shanghai Metro network.

Number of trains	Number of constraints Step 1	Number of variables Step 1	Step 1 CPU time (s)	Number of constraints Step 2	Number of Variable Step 2	Step 2 CPU Time (s)	Initial effective energy consumption (kWh)	Final effective energy consumption (kWh)	Reduction in effective energy consumption
1000	91998	30060	3.24	116,558	34,871	6.03	250951.3	201658.7	19.64%
1032	94944	31022	3.03	120,394	36,038	5.45	261994.5	208558.1	20.40%
1066	98074	32044	3.96	124,494	37,290	5.62	272486.7	215896.7	20.77%
1100	101204	33066	3.47	129,284	38,887	5.39	288677.5	229091.8	20.64%
1132	104150	34028	3.15	133,354	40,171	6.69	308924.4	243672	21.12%
1166	107280	35050	2.84	137,322	41,357	6.67	322612.7	256288.7	20.56%
1198	110226	36012	2.96	141,322	42,606	7.16	329388.2	262205.6	20.40%
1232	113356	37034	4.04	145,756	44,025	7.61	354050.2	277536.7	21.61%
1266	116486	38056	3.84	149,868	45,283	8.74	368901.4	297815	19.27%
1298	119432	39018	3.93	153,480	46,338	7.62	366488.4	293068.8	20.03%
1332	122562	40040	4.22	157,752	47,676	8.02	379700.8	300910.1	20.75%

where a_0, a_1, a_2 are known positive numbers. At time instance τ, the net acceleration of the train is equal to $u_t(\tau) - r(v_t(\tau))$, where $u_t(\tau)$ bounded by magnitude constraints which are non-increasing and depends on the speed of the train. Only the positive acceleration force consumes energy and negative acceleration during braking produces regenerative energy. Define, $u_t^+(\tau) = \max\{0, u_t(\tau)\}$, and $u_t^-(\tau) = \max\{0, -u(\tau)\}$ which represents the positive and negative part of $u_t(\tau)$, respectively. The negative acceleration associated with regenerative braking is denoted by $u_{t,\text{regen}}^-(\tau)$. So, the total energy consumed by the train while making this trip is given by the integral: $\int_0^T m_t u_t^+(\tau)s_t(\tau)d\tau$ and the total regenerative energy produced by the train is given by $\int_0^T m_t u_{t,\text{regen}}^-(\tau)s_t(\tau)d\tau$.

Consider a suitable train pair, say trains t and $\tilde{t}$ associated with the SPSTP $(i, j, t, \tilde{t})$, with train t accelerating and train $\tilde{t}$ braking. After we have calculated the timetable, it will provide us with the duration time during which they are synchronized. Let us denote the times for the beginning and end of the synchronization process by T_1 and T_2. For any $x \in \mathbf{R}$, denote $x^+ = \max\{x, 0\}$. Then the effective energy consumption of associated with this train pair is denoted by,

$$\int_{T_1}^{T_2} \left(m_t u_t^+(\tau)s_t(\tau) - m_{\tilde{t}} u_{\tilde{t},\text{regen}}^-(\tau)s_{\tilde{t}}(\tau) \right)^+ d\tau,$$

The physical interpretation for the above integral is as follows. If for some reason we have more regenerative energy can be provided than needed by accelerating train (though the likelihood of the occurrence of this case is very low in practice), then the extra energy is burned via resistive braking. Similarly we can define the effective energy consumption with train $\tilde{t}$ accelerating and train t braking as follows:

$$\int_{T_1}^{T_2} \left(m_{\tilde{t}} u_{\tilde{t}}^+(\tau)s_{\tilde{t}}(\tau) - m_t u_{t,\text{regen}}^-(\tau)s_t(\tau) \right)^+ d\tau.$$

So, the effective energy consumption effective energy consumption associated with the SPSTP $(i, j, t, \tilde{t})$ is denoted by:

$$E_{\text{effective}}^{(i,j,t,\tilde{t})} = \begin{cases} \int_{T_1}^{T_2} \left(m_t u_t^+(\tau)s_t(\tau) - m_{\tilde{t}} u_{\tilde{t},\text{regen}}^-(\tau)s_{\tilde{t}}(\tau) \right)^+ d\tau, & \text{if train } t \text{ is accelerating and train } \tilde{t} \text{ is braking} \\ \int_{T_1}^{T_2} \left(m_{\tilde{t}} u_{\tilde{t}}^+(\tau)s_{\tilde{t}}(\tau) - m_t u_{t,\text{regen}}^-(\tau)s_t(\tau) \right)^+ d\tau, & \text{if train } t \text{ is braking and train } \tilde{t} \text{ is accelerating} \end{cases}$$

In practice, these integrations are performed numerically for which robust and fast packages exist *e.g.*, Johnson in our case. The total effective energy consumption over all SPSTPs is given by:

$$E_{\text{effective}} = \sum_{(i,j,t,\tilde{t}) \in \mathcal{E}} E_{\text{effective}}^{(i,j,t,\tilde{t})}.$$

The original timetables, which we compare the final timetables with, are provided by Thales Canada Inc. It should be noted that, the number of trains $\mathcal{T}$ is fixed for each of the instances. The energy calculation is done using SPSIM, which is a proprietary software owned by Thales Canada Inc (Vlad and Tatarnikov, 2011), and Cubature, which is an open-source Julia package written by Steven G. Johnson that uses an adaptive algorithm for the approximate calculation of multiple integrals Johnson. SPSIM calculates the power versus time graphs of all the active trains for the original and optimal timetables. Cubature is used to calculate the effective area under the power versus time graphs to determine 1) the total energy required by the trains during the trips, 2) the total transferred regenerative energy during the SPSTPs, and 3) the effective energy consumption as the difference of the first two quantities. The effective energy consumption of the optimal timetables in comparison with the original ones is reduced quite significantly - even in the worst case, the reduction in effective energy consumption is 19.27%, with the best case corresponding to 21.61%.

8. Conclusion

In this paper we have proposed a novel two-step linear optimization model to calculate an energy-efficient timetable in modern metro railway networks. The objective is to minimize the total electrical energy consumption of all trains and to maximize the utilization of regenerative energy produced by braking trains. In contrast to other existing models, this model is computationally the most tractable one. We have applied our optimization model to eleven different instances of service PES2-SFM2 of line 8 of Shanghai Metro network. All instances span the full service period of one day (18 hours) with thousands of active trains. For all instances our model has found optimal timetables in less than 13s with significant reductions in the effective energy consumption. Code based on our optimization model has been integrated with the industrial timetable compiler of Thales Inc.

Acknowledgments

Appendix

Table 3
Speed limit for line 8 of Shanghai metro network.

Origin-destination	Start (m)	End (m)	Speed limit (km/h)
CSR1-YSS1	0.0	143.5	60
	143.5	1004.6	70
	1004.6	1138.2	60
CSR2-YHR2	0.0	910.0	60
GRW1-LXM1	0.0	153.3	60
	153.3	870.1	70
	870.1	1006.9	60
GRW2-PES2	0.0	173.1	60
	173.1	636.4	70
	636.4	769.5	60
JYR1-LZV1	0.0	1366.7	60
	1366.7	2220.6	65
	2220.6	2357.3	60
JYR2-YSS2	0.0	143.4	60
	143.4	1388.9	70
	1388.9	1522.3	60
JYS1-LHS1	0.0	140.0	60
	140.0	829.2	75
	829.2	1202.3	60
JYS2-PJT2	0.0	140.0	60
	140.0	371.1	70
	371.1	1081.9	75
	1081.9	1249.8	70
	1249.8	1386.2	60
LHR1-PJT1	0.0	140.1	60
	140.1	766.2	70
	766.2	1623.4	75
	1623.4	1805.9	70
	1805.9	2374.4	75
	2374.4	2487.8	70
	2487.8	2624.3	60
LHR2-LZV2	0.0	139.8	60
	139.8	2457.3	70
	2457.3	2594.1	60
LHS1-SFM1	0.0	140.0	60
	140.0	1220.1	70
	1220.1	1357.4	60
LHS2-JYS2	0.0	186.7	60
	186.7	853.8	75
	853.8	1064.4	70
	1064.4	1200.8	60
LJB1-SXZ1	0.0	140.1	60
	140.1	1027.4	70
	1027.4	1167.2	60

Table 3 (*continued*)

Origin-destination	Start (m)	End (m)	Speed limit (km/h)
LJB2-LXM2	0.0	140.1	60
	140.1	693.3	70
	693.3	830.2	60
LXM1-LJB1	0.0	140.0	60
	140.0	689.3	70
	689.3	826.1	60
LXM2-GRW2	0.0	140.0	60
	140.0	855.5	70
	855.5	1005.2	60
LZV1-LHR1	0.0	140.1	60
	140.1	1901.1	70
	1901.1	2199.1	75
	2199.1	2456.3	70
	2456.3	2592.8	60
LZV2-JYR2	0.0	143.3	60
	143.3	1007.8	65
	1007.8	2338.1	60
PES1-GRW1	0.0	140.0	60
	140.0	561.7	70
	561.7	761.5	60
PJT1-JYS1	0.0	143.3	60
	143.3	374.6	70
	374.6	1089.8	75
	1089.8	1250.2	70
	1250.2	1386.7	60
PJT2-LHR2	0.0	143.4	60
	143.4	355.8	70
	355.8	829.3	75
	829.3	1039.2	70
	1039.2	1858.3	75
	1858.3	2488.9	70
	2488.9	2622.1	60
SFM2-LHS2	0.0	140.3	60
	140.3	373.0	70
	373.0	742.3	75
	742.3	1225.1	70
	1225.1	1358.3	60
SXZ1-ZJD1	0.0	140.1	60
	140.1	647.2	65
	647.2	1699.3	70
	1699.3	2039.3	60
SXZ2-LJB2	0.0	160.1	60
	160.1	1027.5	70
	1027.5	1164.2	60
YHR1-CSR1	0.0	143.4	60
	143.4	773.7	70
	773.7	910.3	60
YHR2-ZJD2	0.0	140.0	60
	140.0	601.3	70
	601.3	738.0	60
YSS1-JYR1	0.0	140.2	60
	140.2	664.7	70
	664.7	987.7	75
	987.7	1389.2	70
	1389.2	1525.9	60
YSS2-CSR2	0.0	430.4	60
	430.4	1014.8	70
	1014.8	1151.6	54
ZJD1-YHR1	0.0	140.1	60
	140.1	605.9	70
	605.9	742.5	60
ZJD2-SXZ2	0.0	353.8	60
	353.8	1393.7	70
	1393.7	1910.0	65
	1910.0	2043.3	60

References

Albrecht, A., Howlett, P., Pudney, P., Vu, X., Zhou, P., 2015. The key principles of optimal train control - part 1: formulation of the model, strategies of optimal type, evolutionary lines, location of optimal switching points. Transp. Res. Part B.

Avinash Balakrishnan, K.S. (Ed.)2014. In: Nanostructured Ceramic Oxides for Supercapacitor Applications. CRC Press.

Bashash, S., Moura, S.J., Forman, J.C., Fathy, H.K., 2011. Plug-in hybrid electric vehicle charge pattern optimization for energy cost and battery longevity. J. Power Sources 196 (1), 541–549.

Boyd, S., Vandenberghe, L., 2009. Convex Optimization. Cambridge university press.

Calafiore, G., El Ghaoui, L., 2014. Optimization Models. Cambridge University Press.

Ciccarelli, F., Del Pizzo, A., Iannuzzi, D., 2014. Improvement of energy efficiency in light railway vehicles based on power management control of wayside lithium-ion capacitor storage. IEEE Trans. Power Electr. 29 (1), 275–286.

Das Gupta, S., Pavel, L., Kevin Tobin, J., 2015. An optimization model to utilize regenerative braking energy in a railway network. In: American Control Conference (ACC).

Davis, W.J., 1926. The Tractive Resistance of Electric Locomotives and Cars, vol. 29. General Electric Review.

Droste-Franke, B., Paal, B., Rehtanz, C., Sauer, D.U., Schneider, J.-P., Schreurs, M., Ziesemer, T., 2012. Balancing Renewable Electricity: Energy Storage, Demand Side Management, and Network Extension from an Interdisciplinary Perspective, vol. 40. Springer Science & Business Media.

González-Gil, A., Palacin, R., Batty, P., 2013. Sustainable urban rail systems: Strategies and technologies for optimal management of regenerative braking energy. Ener. Conversion Manage. 75, 374–388.

Group, S. S. M., 2015. Description of line 8, shanghai metro.

Harrod, S.S., 2012. A tutorial on fundamental model structures for railway timetable optimization. Surv. Oper. Res. Manage. Sci. 17 (2), 85–96.

Howlett, P., 2000. The optimal control of a train. Ann. Oper. Res. 98 (1–4), 65–87.

Howlett, P.G., Pudney, P.J., 1995. Energy-Efficient Train Control. Springer Science & Business Media.

Howlett, P.G., Pudney, P.J., Vu, X., 2009. Local energy minimization in optimal train control. Automatica 45 (11), 2692–2698.

Jiaxin, C., Howlett, P., 1993. A note on the calculation of optimal strategies for the minimization of fuel consumption in the control of trains. IEEE Trans. Autom. Control 38 (11), 1730–1734.

Johnson, S. G.,. The cubature module for julia. [Online]. Available: https://github.com/stevengj/Cubature.jl.

Kapadia, A.S., Chan, W., Moyé, L.A., 2005. Mathematical Statistics with Applications. CRC Press.

Khmelnitsky, E., 2000. On an optimal control problem of train operation. IEEE Trans. Autom. Control 45 (7), 1257–1266.

Le, Z., Li, K., Ye, J., Xu, X., 2014. Optimizing the train timetable for a subway system. Proceedings of the Institution of Mechanical Engineers, Part F: Journal of Rail and Rapid Transit doi:10.1177/0954409714524377.

Li, X., Lo, H.K., 2014a. An energy-efficient scheduling and speed control approach for metro rail operations. Transp. Res. Part B 64, 73–89.

Li, X., Lo, H.K., 2014b. Energy minimization in dynamic train scheduling and control for metro rail operations. Transp. Res. Part B 70, 269–284.

Liebchen, C., 2007. Periodic timetable optimization in public transport. Springer.

Liu, R.R., Golovitcher, I.M., 2003. Energy-efficient operation of rail vehicles. Transp. Res. Part A 37 (10), 917–932.

Lubin, M., Dunning, I., 2015. Computing in operations research using julia. INFORMS J. Comput. 27 (2), 238–248. doi:10.1287/ijoc.2014.0623.

Mahajan, S., 2010. Street-Fighting Mathematics. MIT Press Cambridge.

Mendenhall, W., Beaver, R., Beaver, B., 2009. Introduction to probability and statistics. Cengage Learning.

Milroy, I.P., 1980. Aspects of Automatic Train Control. Ph.D. thesis Loughborough University of Technology.

Mura, R., Utkin, V., Onori, S., 2013. Recasting the hev energy management problem into an infinite-time optimization problem including stability. In: Proceedings of IEEE 52nd Annual Conference on Decision and Control (CDC), pp. 6837–6842.

Nuesch, T., Ott, T., Ebbesen, S., Guzzella, L., 2012. Cost and fuel-optimal selection of hev topologies using particle swarm optimization and dynamic programming. In: Proceedings of American Control Conference (ACC), pp. 1302–1307.

Patil, R., Kelly, J.C., Filipi, Z., Fathy, H., 2012. A framework for the integrated optimization of charging and power management in plug-in hybrid electric vehicles. In: Proceedings of American Control Conference (ACC), pp. 1327–1334.

Peeters, L., 2003. Cyclic Railway Timetable Optimization. Ph.D. thesis Erasmus University Rotterdam.

Peña-Alcaraz, M., Fernández, A., Cucala, A.P., Ramos, A., Pecharromán, R.R., 2012a. Optimal underground timetable design based on power flow for maximizing the use of regenerative-braking energy. Proceedings of the Institution of Mechanical Engineers, Part F: Journal of Rail and Rapid Transit 226 (4), 397–408.

Peña-Alcaraz, M., Webster, M., Ramos, A., 2012b. An approximate dynamic programming approach for designing train timetables. ESD Working Paper Series.

Saber, A.Y., Venayagamoorthy, G.K., 2010. Intelligent unit commitment with vehicle-to-grid: A cost-emission optimization. J. Power Sources 195 (3), 898–911.

Schrijver, A., 1998. Theory of Linear and Integer Programming. John Wiley & Sons.

Vlad, E.P., Tatarnikov, V., 2011. R&M&A&S of communication based train control systems applied to urban rail transportation way to improve city sustainability. In: Proceedings of IEEE Reliability and Maintainability Symposium (RAMS), pp. 1–6.

Yang, X., Li, X., Gao, Z., Wang, H., Tang, T., 2013. A cooperative scheduling model for timetable optimization in subway systems. IEEE Trans. Intell. Transp. Syst. 14 (1), 438–447.

Further reading

Bombardier Inc., 2010. Energstor wayside energy storage. [Online]. Available: http://www.bombardier.com/content/dam/Websites/bombardiercom/supporting-documents/BT/Bombardier-Transportation-ECO4-EnerGstor-EN.pdf.

Lu, M., Beguin, F., Frackowiak, E., 2013. Supercapacitors: Materials, Systems and Applications. John Wiley & Sons.